

A Novel Controller Based on Single-Phase Instantaneous p-q Power Theory for a Cascaded PWM Transformerless STATCOM for Voltage Regulation

M. Abbasi, B. Tousi*

Department of Electrical Engineering, Urmia University, Urmia, Iran.

Abstract- In this paper, dynamic performance of a transformerless cascaded PWM static synchronous shunt compensator (STATCOM) based on a novel control scheme is investigated for bus voltage regulation in a 6.6kV distribution system. The transformerless STATCOM consists of a thirteen-level cascaded H-bridge inverter, in which each voltage source H-bridge inverter should be equipped with a floating and isolated capacitor without any power source. The proposed control algorithm uses instantaneous p-q power theory in an innovative way that devotes itself not only to meet the reactive power demand but also to balance the dc link voltages at the same time. DC link voltage balancing control consists of two main parts: cluster and individual balancing. The control algorithm based on a phase shifted carrier modulation strategy has no restriction on the number of cascaded voltage source H-bridge inverters. Comprehensive simulations are presented in MATLAB/ SIMULINK environment for validating the performance of proposed transformerless STATCOM.

Keyword: Cascaded H-Bridge inverter, DC link voltage balancing, p-q theory, Transformerless STATCOM.

1. INTRODUCTION

FACTS (Flexible AC Transmission System) devices are power electronics based reactive power compensators that can provide ability to make quick adjustments and to control modern complex electrical system. They can be connected in series, in parallel, or in a combination of both. Shunt compensation based on voltage source inverter, known as STATCOM, is a shunt connected FACTS device for absorbing or generating reactive power. It generates a set of three phase sinusoidal voltages at the fundamental frequency, with quickly controllable amplitude and phase angle. FACTS devices can perform functions such as voltage regulation, power factor correction, sub synchronous resonance mitigation and power oscillation damping, etc. [1-5].

Multilevel inverters have several advantages over other inverters as lower common mode voltage, lower voltage stress on switches and lower distortion in output voltage and current [6-8]. Because of these

remarkable advantages, multilevel inverters have attracted wide interest of researchers in recent years. The most famous multilevel structures are classified as: diode clamped, flying capacitor, cascaded H-bridge. Among these topologies, cascaded H-bridge inverter that is used in proposed transformerless STATCOM, has a modular structure and needs least number of power devices compared to other two topologies. Cascaded H-bridge inverter consists of series connection of voltage source H-bridge inverters. Each of these H-bridge inverters must be equipped with a floating and isolated dc capacitor without any additional power sources. However, cascaded H-bridge inverter suffers from an imbalance between dc link voltages that is caused by unequal conducting and switching losses of power switches, passive components tolerances and imbalances and resolution issues inherent in the control circuit [9].

Besides the developments of multilevel inverters topologies, advances in the area of power electronic switches led to very high power and frequency switches as insulated gate bipolar transistors (IGBTs) and gate turn-off thyristors (GTOs), which in turns led to multilevel inverters with higher ratings. Because of these advances, elimination of the transformer, as the link of power system and FACTS devices, has been state of art in recent years [9-14]. Mostly, researchers

Received: 10 Apr. 2017

Revised: 21 Jun. 2017

Accepted: 19 Oct. 2017

*Corresponding author:

E-mail: b.tousi@urmia.ac.ir (Behrouz Tousi)

Digital object identifier: 10.22098/joape.2018.3491.1278

© 2018 University of Mohaghegh Ardabili. All rights reserved.

have been interested in transformerless STATCOM in medium voltage applications [9-12].

The transformerless FACTS devices offer several advantages over the conventional technology such as low cost, small size, light weight, high efficiency and fast dynamic response [14]. Therefore, they can be installed and used widely in power systems, which in turns will enhance the controllability, reliability and stability of power systems and will provide an increased possibility to use more renewable sources like wind and solar in power systems. The increase of solar and wind energy has been recognized as a global awareness because of global warming and fossil fuels exhaustion [14-16]. In addition, this increase has also a negative effect on the power networks in terms of voltage control, frequency regulation, transient stability and oscillation damping [14,16]. Thus, the development and installation of transformerless FACTS devices is a suitable solution for these technical challenges.

The proposed control algorithm is founded on instantaneous p-q power theory which has been introduced by Akagi, Kanazawa and Nabae in 1983 [17,18]. This theory is based on instantaneous values in three-phase systems with or without neutral wire and is applicable in transient and steady state operations. In this paper, this theory is defined and used for each phase separately, hereafter called "single-phase instantaneous p-q power theory". In previous conventional methods based on instantaneous p-q theory [19, 20], the reference shunt current that should be generated by the compensator has been calculated using the instantaneous p-q power theory and then the switching pulses have been generated by the hysteresis band control. However it is the first time that the generated reference current by the instantaneous p-q power theory goes again through the same theory to generate reference voltages. In proposed method, we can use the PS PWM method for generating the switching pulses which is one of the well-known methods that has many advantages over other switching methods especially in STATCOM including multilevel inverters.

2. TEST SYSTEM AND STATCOM OPERATING PRINCIPLES

Single-phase diagram of system configuration is shown in Fig. 1, which consists of a three-phase source (V_s), an equivalent series reactance (X_L), a

transformerless STATCOM and a three-phase balanced load. As shown in Fig. 1, transformerless STATCOM includes a complete digital control system and a cascaded H-bridge inverter, which is connected to the bus through a reactance (X_{sh}).

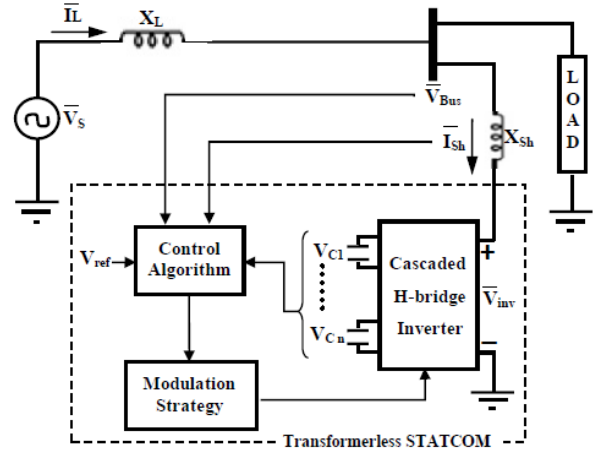


Fig. 1. Single-phase diagram of system configuration

In order to demonstrate voltage regulation using the proposed transformerless STATCOM, the output voltage of cascaded H-bridge inverter is introduced by V_{inv} with a phasor angle ϕ_{inv} and the bus voltage is introduced by V_{Bus} with a phasor angle ϕ_{Bus} , as shown in Fig. 2. Therefore, the active and reactive power that transformerless STATCOM injects to the bus, can be written as shown in below:

$$P_{inv} = \frac{V_{inv} V_{Bus} \sin(\phi_{inv} - \phi_{Bus})}{X_{sh}} \quad (1)$$

$$Q_{inv} = \frac{V_{inv}^2 - V_{inv} V_{Bus} \cos(\phi_{inv} - \phi_{Bus})}{X_{sh}} \quad (2)$$

As mentioned, transformerless STATCOM is a shunt compensator based on voltage source inverter without any power source, which only exchanges reactive power ($P_{in}=0$). This means that V_{inv} and V_{Bus} are in phase ($\phi_{inv}=\phi_{Bus}$) and therefore, the injected reactive power to the bus can be written as below:

$$Q_{inv} = \frac{V_{inv}^2 - V_{inv} V_{Bus}}{X_{sh}} \quad (3)$$

According to Eq. (3), increasing amplitude of cascaded H-bridge inverter terminal voltage above amplitude of the bus voltage causes capacitive current to be injected into the bus.

In general, STATCOM can be considered as a controllable shunt capacitance in capacitive position

for increasing bus voltage and as a controllable shunt inductance in inductive position for bus voltage decrement.

3. TRANSFORMERLESS STATCOM DESIGN

The calculation of cascaded H-bridge inverter components is done in the following order. Given the transformerless STATCOM MVA rating and voltage rating, the required dc link voltage is determined assuming a linking reactance of 10%. At following, rated phase voltage amplitude of system and rated apparent power of transformerless STATCOM are assumed as the base voltage and the base power. Next, the inverters rated current is determined. Then, "cascade number" is calculated, which refers to the number of cascaded voltage source H-bridge inverters in each phase. Finally, a sizing method for dc link floating capacitors is presented which keeps the peak-to-peak dc link voltage ripple to 10%.

Maximum dc link voltage is the voltage, which is required to generate rated leading current into rated bus voltage:

$$V_{DC,max} = \left[\frac{2}{m_0} \right] \left[V_{bus,rated} (X_{Link(pu)} + 1) \right] \quad (4)$$

Where m_0 is the modulation index and $X_{Link(pu)}$ is per unit value of the linking reactance. Moreover, rated phase current amplitude of inverters can be obtained as below:

$$|I_{sh,rated}| = \frac{2}{3} \left[\frac{S_{Base}}{V_{Base}} \right] \quad (5)$$

Now a day, very high power switches as GTOs and IGBTs are commercially available [9-14]. Therefore, it is possible to build the H-bridge inverters with rated values about $2kV$ $125A$. This gives the cascade number, as shown below:

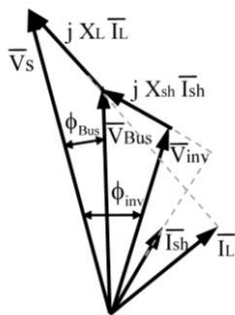


Fig. 2. Vector diagram for STATCOM operation

$$n = \frac{V_{DC,max}}{V_{HB,max}} = \frac{11.8kV}{2kV} \cong 6 \quad (6)$$

Circuit configuration of the transformerless STATCOM cascading six H-bridge PWM inverter is shown in Fig. 3, where $V_{HB,n}$ is output voltage of nth H-bridge inverter. All the power switches have the same voltage and current ratings.

For each H-bridge inverter, the minimum floating dc link capacitor can be calculated based on the maximum permissible ripples on top of the dc link voltage [10], as shown below:

$$C_{HB} = \frac{1.6 |I_{sh,rated}|}{f_c \Delta V_{C,max}} \quad (7)$$

Where $\Delta V_{C,max}$ is maximum acceptable ripple on dc link voltages and f_c is the carrier frequency.

4. CONTROL SYSTEM

4.1. Control Algorithm

Block-diagram of proposed control algorithm is shown in Fig. 4, in which the single-phase instantaneous p-q theory has been used successively for achieving desired purposes.

As well as, Fig. 5 presents the block diagrams of single-phase instantaneous p-q power theory which are used in this paper. As shown in Fig. 5, single-phase instantaneous p-q theory has two types of input and output signals. First, voltage, active power and reactive power are the input signals and the output signal is current, as shown in Fig. 5a. Second, the input signals are current, active power and reactive power and the output signal is voltage, as presented in Fig. 5b.

At the first step, meeting the reactive power demand is considered. As shown in Fig. 5a, by

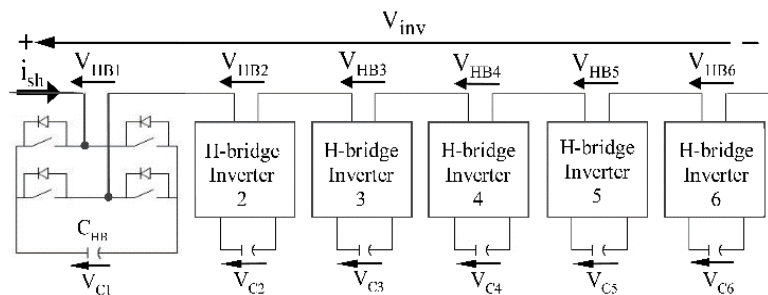


Fig. 3. Circuit configuration of cascading six H-bridge PWM inverter (cluster)

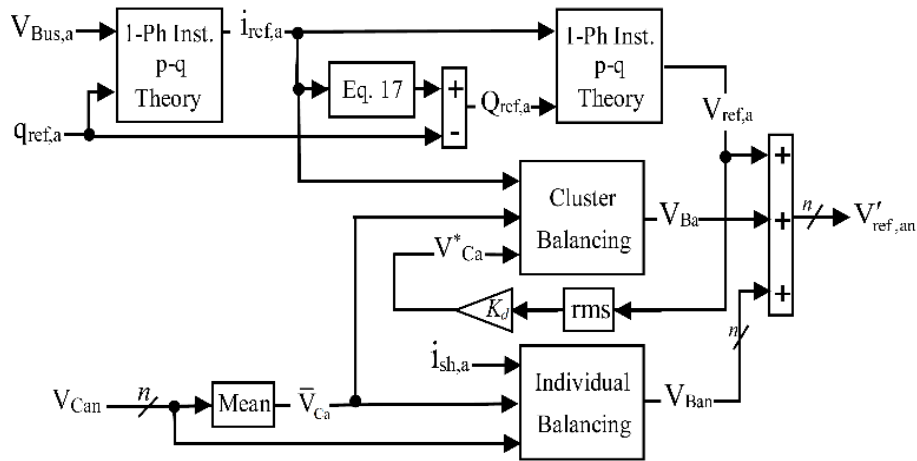


Fig. 4. Proposed control algorithm

considering input signals as instantaneous bus voltage (V_{Bus}) and required reactive power, reference shunt current that should flow in shunt branch can be obtained as output signal. At following, calculations are performed for a-phase. Generally, a-phase bus voltage can be assumed as:

$$v_{Bus,a}(t) = V \sin(\omega t + \theta_v) \quad (8)$$

Equation (8) can be transformed in matrix form as follows:

$$\begin{bmatrix} v_a^* \\ v_b^* \\ v_c^* \end{bmatrix} = \begin{bmatrix} 1 \\ 1\angle 120^\circ \\ 1\angle 240^\circ \end{bmatrix} v_{Bus,a} \quad (9)$$

Using Clarke transformation, a - b - c coordinates of voltage matrix can be transformed into α - β coordinates:

$$\begin{bmatrix} v_\alpha^* \\ v_\beta^* \end{bmatrix} = \sqrt{\frac{2}{3}} \begin{bmatrix} 1 & -1 & -1 \\ 0 & \sqrt{3} & -\sqrt{3} \end{bmatrix} \begin{bmatrix} v_a^* \\ v_b^* \\ v_c^* \end{bmatrix} \quad (10)$$

According to the instantaneous p-q power theory, instantaneous real and imaginary power is written as shown in below:

$$\begin{bmatrix} p \\ q \end{bmatrix} = \begin{bmatrix} v_\alpha^* & v_\beta^* \\ -v_\beta^* & v_\alpha^* \end{bmatrix} \begin{bmatrix} i_\alpha^* \\ i_\beta^* \end{bmatrix} \quad (11)$$

Now, by inverting (11), α - β coordinate of currents matrix will be calculated:

$$\begin{bmatrix} i_\alpha^* \\ i_\beta^* \end{bmatrix} = \frac{1}{v_\alpha^{*2} + v_\beta^{*2}} \begin{bmatrix} v_\alpha^* & v_\beta^* \\ -v_\beta^* & v_\alpha^* \end{bmatrix} \begin{bmatrix} p \\ q \end{bmatrix} \quad (12)$$

Then by inverse Clark transformation, a - b - c coordinates of currents can be obtained as:

$$\begin{bmatrix} i_a^* \\ i_b^* \\ i_c^* \end{bmatrix} = \sqrt{\frac{2}{3}} \begin{bmatrix} 1 & 0 \\ -1/2 & \sqrt{3}/2 \\ -1/2 & -\sqrt{3}/2 \end{bmatrix} \begin{bmatrix} i_\alpha^* \\ i_\beta^* \end{bmatrix} \quad (13)$$

Moreover, with same definition used in Eq. (9), current matrix can be written as:

$$\begin{bmatrix} i_a^* \\ i_b^* \\ i_c^* \end{bmatrix} = \begin{bmatrix} 1 \\ 1\angle 120^\circ \\ 1\angle 240^\circ \end{bmatrix} i_{ref,a} \quad (14)$$

Finally, a-phase reference compensation shunt current can be expressed as below:

$$i_{ref,a} = \sqrt{\frac{2}{3}} \left(\frac{v_\alpha^*}{v_\alpha^{*2} + v_\beta^{*2}} p + \frac{v_\beta^*}{v_\alpha^{*2} + v_\beta^{*2}} q \right) \quad (15)$$

Where q and p are reference instantaneous reactive and real power that should be generated by proposed compensator at the bus point. Ideally, the

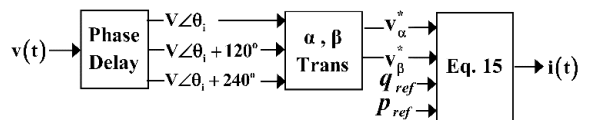


Fig. 5a

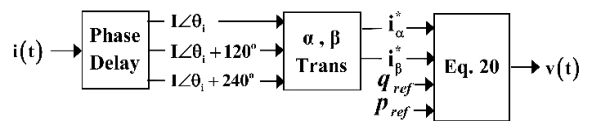


Fig. 5b

Fig. 5. Block diagram of single-phase instantaneous p-q power theory when output signal is (a) current (b) voltage

compensator is designed to produce or absorb only reactive power, thus:

$$q = q_{ref,a} \quad , \quad p = 0 \quad (16)$$

In some papers [19,20], the shunt branch current (i_{sh}) is controlled using some control methods like hysteresis band control after obtaining the reference shunt current. However, this goal is achieved by reusing the single-phase instantaneous p-q theory in this paper. Absorbed reactive power by shunt equivalent reactance (X_{sh}) under the reference shunt current can be obtained as below:

$$q_{X,a} = X_{sh} |i_{ref,a}|^2 \quad (17)$$

Thus, the reference reactive power, which should be generated at the terminal of transformerless cascaded H-bridge inverter, can be calculated as follow:

$$Q_{ref,a} = q_{ref,a} + q_{X,a} \quad (18)$$

Now, the reference voltage of transformerless STATCOM should be calculated, which is required for generating the reference shunt current. As shown in Fig. 5b, by presuming $Q_{ref,a}$ and $i_{ref,a}$ from Eqs. (15), (16) and (18), as input signals for single-phase instantaneous p-q theory, the reference voltage will be obtained as output signal. Assume that $i_{ref,a}$ is a sinusoidal signal:

$$i_{ref,a}(t) = I \cos(\omega t + \theta_1) \quad (19)$$

Using single-phase instantaneous p-q theory, which includes the same process that is performed during Eqs. (8)-(15), the reference voltage of transformerless STATCOM can be expressed as:

$$V_{ref,a} = \sqrt{\frac{2}{3}} \left(\frac{i_{\alpha}^*}{i_{\alpha}^{*2} + i_{\beta}^{*2}} p' - \frac{i_{\beta}^*}{i_{\alpha}^{*2} + i_{\beta}^{*2}} q' \right) \quad (20)$$

Where q' and p' are total reference reactive and active power that must be generated at transformerless STATCOM terminal. As mentioned, the transformerless STATCOM is designed to exchange only reactive power, therefore:

$$q' = Q_{ref,a} \quad , \quad p' = 0 \quad (21)$$

For maintaining the bus voltage amplitude, it will be desired to deregulate the reactive power reference respect to bus voltage amplitude deviations from rated value. Therefore, total reference reactive power

that should be generated at transformerless STATCOM terminal can be written as below:

$$Q_{ref,a} = \left(K_p + \frac{K_i}{s} \right) \Delta |V_{Bus,a}| + q_{meas,a} + q_{X,a} \quad (22)$$

Where $\Delta |V_{Bus,a}|$ is the deviation of bus voltage amplitude from the rated value and $q_{meas,a}$ is instantaneously measured reactive power that exchanges at the bus point.

4.2. Voltage Balancing

The cascaded H-bridge inverter used in transformerless STATCOM comprises series connection of six H-bridge inverters. Thus, for controlling fundamental component of total output voltage, each capacitor should be charged or discharged accurately to modify the dc link voltages. As mentioned, proposed voltage balancing control has two main parts: cluster and individual balancing. Attention is paid to the a-phase in the following.

4.2.1. Cluster Balancing

Figure 6 shows block diagram of proposed cluster balancing control considering each phase cascaded H-bridge inverter as a unified H-bridge inverter. A low pass filter with a cut off frequency of 15Hz is used to eliminate the 120Hz (double line frequency) component from the detected dc voltages. Required active power for cluster balancing control (\bar{p}_a) is yielded from the average value of dc link voltages (\bar{V}_{Ca}) and common dc link voltage reference (V_C^*) as expressed below:

$$\bar{V}_{Ca} = \frac{\sum_{n=1}^6 V_{Can}}{6} \quad (23)$$

$$\bar{p}_a = (V_C^* - \bar{V}_{Ca}) \left(K_p' + \frac{K_i'}{s} \right) \quad (24)$$

Where \bar{p}_a is the real power that should be absorbed or generated by H-bridge inverters for charging or discharging their capacitors. As shown in Fig. 5b, by using single-phase instantaneous p-q theory, with input signals of i_{ref} and \bar{p}_a , cluster balancing control signal (V_{Ba}) can be obtained as:

$$V_{Ba} = \sqrt{\frac{2}{3}} \left(\frac{i_{\alpha}^*}{i_{\alpha}^{*2} + i_{\beta}^{*2}} \bar{p}_a \right) \quad (25)$$

This control signal makes a phase difference between reference voltage of cascaded H-bridge inverter and bus voltage; therefore, a controlled active power can be exchanged, which in turns will balance the average value of dc link voltages.

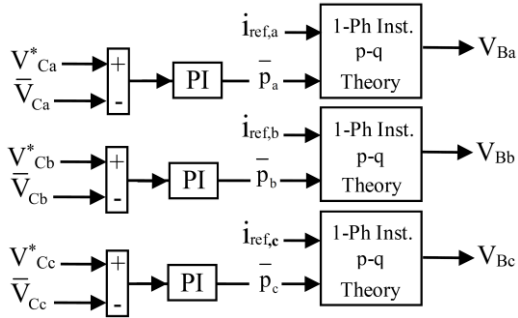


Fig. 6. Proposed cluster balancing control

4.2.2. Individual balancing

Figure 7 shows the proposed individual voltage balancing between the six H-bridge inverters of a-phase cluster. This control signal must be enough smaller than cluster balancing control signal for avoiding a conflict of control between the two control signal. The required active power for individual balancing control of n th H-bridge inverter (P_{Can}) is yielding from the average value of dc link voltages (\bar{V}_{Ca}) and dc link voltage of n th H-bridge inverter (V_{Can}) as shown in below:

$$P_{Can} = (\bar{V}_{Ca} - V_{Can}) \left(K_p^n + \frac{K_i^n}{s} \right) \quad (26)$$

Then by using single-phase instantaneous p-q theory, as shown in Fig. 5b, with input signals of measured shunt current $i_{sh,a}$ and P_{Can} , individual balancing control signal (V_{Ban}) can be obtained as:

$$V_{Ban} = \sqrt{\frac{2}{3}} \left(\frac{i_\alpha^*}{i_\alpha^{*2} + i_\beta^{*2}} P_{Can} \right) \quad (27)$$

According to Eqs. (22), (27) and (29), reference voltages of n th H-bridge inverter can be defined as follows:

$$V'_{ref,an} = V_{ref,a} + V_{Ba} + V_{Ban} \quad (28)$$

$$V'_{ref,bn} = V_{ref,b} + V_{Bb} + V_{Bbn} \quad (29)$$

$$V'_{ref,cn} = V_{ref,c} + V_{Bc} + V_{Bcn} \quad (30)$$

These reference voltages are applied directly to modulation strategy for generating the switching pulses.

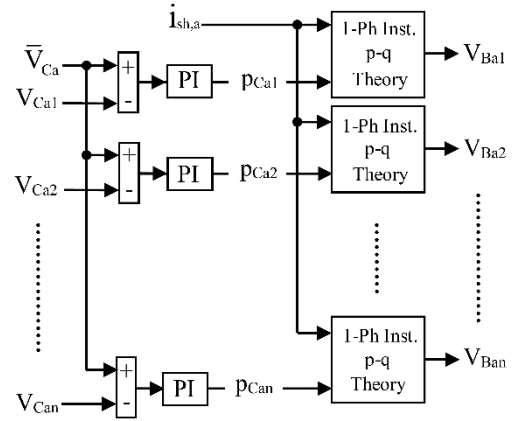


Fig. 7. Proposed individual balancing control

4.3 Modulation Strategy

Proposed modulation strategy is shown in Fig. 8, which is so-called "Phase Shifted PWM". Each H-bridge inverter can be controlled with two independent 2-level pulse patterns.

The phase shifted PWM with same carrier frequency of 1000Hz is applied to cascaded H-bridge inverters. A carrier phase shift of 30° is introduced across the adjacent H-bridge inverters to produce a thirteen-level line-to-neutral output voltage with lowest distortion, because the equivalent switching frequency (f_{Eq}) is twelve times higher than switching frequency per power switches:

$$f_{Eq} = (2 \times f_c) \times 6 = 12 \times f_c = 12\text{kHz} \quad (31)$$

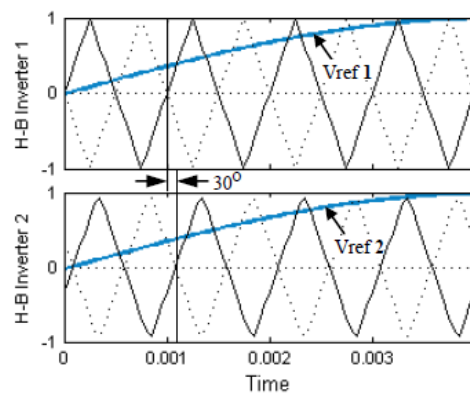


Fig. 8. PS PWM modulation strategy

5. SIMULATION RESULTS

The performance of proposed transformerless cascade PWM STATCOM for bus voltage regulation was simulated using MATLAB Simulink. It is assumed that rated bus voltage amplitude is 5389V , which must be maintained despite load changes. The

load is balanced. Specification of test system used for simulation is shown in Table 1.

Table 1. Specification and parameters used for simulation

Parameters	Symbol	Values
Sending end voltage source	V_s	6.6 kV
Rated bus voltage Amplitude	$V_{Bus, rated}$	5389 V
Rated source current	$I_{L, rms}$	192.1 A
Rated real power of line	P_N	1.5 MVA
Equivalent series impedance	X_L	14.52 Ohms
Load impedance 1	Z_1	$329.3 \angle 2.4^\circ$
Load impedance 2	Z_2	$340.7 \angle -15^\circ$
Power system frequency	f_s	60Hz
Rated reactive power of transformerless STATCOM	Q_{sh}	1 MVA
Rated current of each H-bridge inverter	I_{HB}	124A
Cascade number	n	6
Maximum DC-Link voltage of each H-bridge inverter	$V_{C, Max}$	1.98 kV
DC-Link floating capacitor	C_{HB}	1mF
Carrier frequency	f_c	1 kHz
Modulation index	m_0	1
Equivalent shunt reactance	X_{sh}	47.9 Ohms

Because of the ohmic-inductive properties of loads in power systems, reactive power compensators are mostly used in capacitive mode. Thus, the performance of proposed transformerless STATCOM is validated for capacitive modes by step changes in load. Fig. 9 shows a-phase cluster output voltage ($V_{inv,a}$), bus voltage ($V_{Bus,a}$), and shunt current ($90^\circ I_{sh}$) in maximum capacitive mode. In addition, FFT analysis show acceptable THDs of 4.53% for $V_{inv,a}$, 0.81% for $V_{Bus,a}$ and 1.87% for $I_{sh,a}$, as presented in Fig. 10.

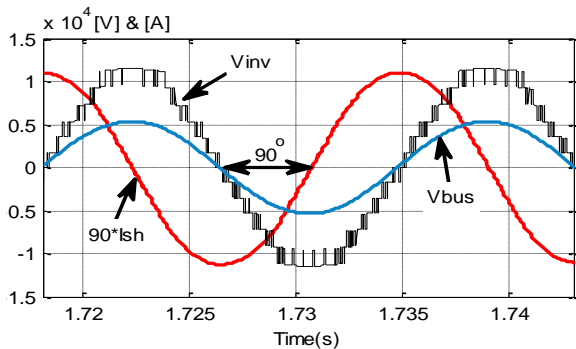


Fig. 9. a-phase cluster output voltage (V_{inv}), bus voltage (V_{Bus}) and shunt current ($90^\circ I_{sh}$)

Figure 11 shows the active and reactive power that are exchanged at the bus point under load changes. It is clear that the absorbed active power by transformerless STATCOM is negligible compared to its injected reactive power to the bus. The amplitude of bus voltages are shown with and without reactive

power compensation in Fig. 12, which clearly validate the voltage regulation capability of transformerless STATCOM based on proposed control scheme.

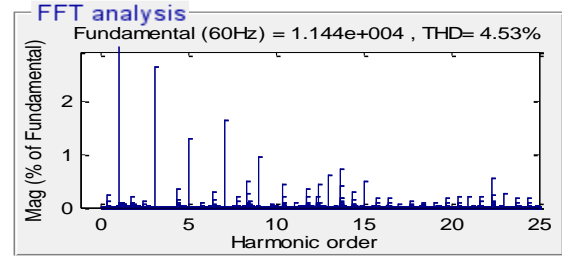


Fig. 10a

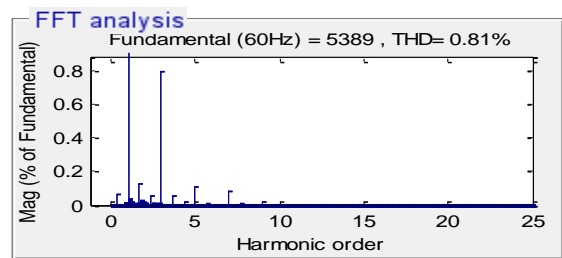


Fig. 10b

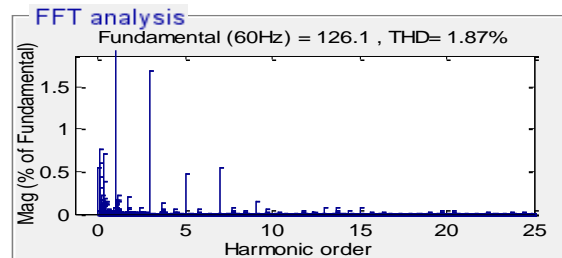


Fig. 10c

Fig. 10. FFT analysis of (a) $V_{inv,a}$ (b) $V_{Bus,a}$ (c) $I_{sh,a}$

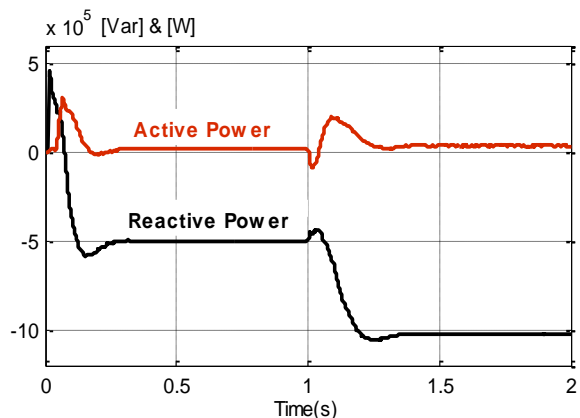


Fig. 11. Three-phase exchanged active and reactive power at the bus point

Figure 13 shows the amplitudes of source current, shunt branch current and load current under the system changes. In addition, waveforms of the a-phase cluster output voltage, bus voltage and shunt current are presented for transient conditions (step

change of load at $t=1s$ in Fig. 14, Fig. 15 and Fig. 16, respectively. Performance of proposed dc link voltage balancing control is proved in Fig. 17. Fig. 17a shows successfully balanced dc link voltages of a-phase cluster with maximum allowable ripples (about 10%).

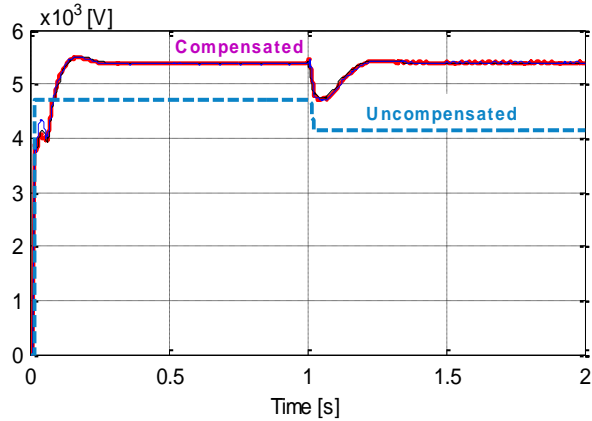


Fig. 12. Bus voltage amplitudes with and without reactive power compensation

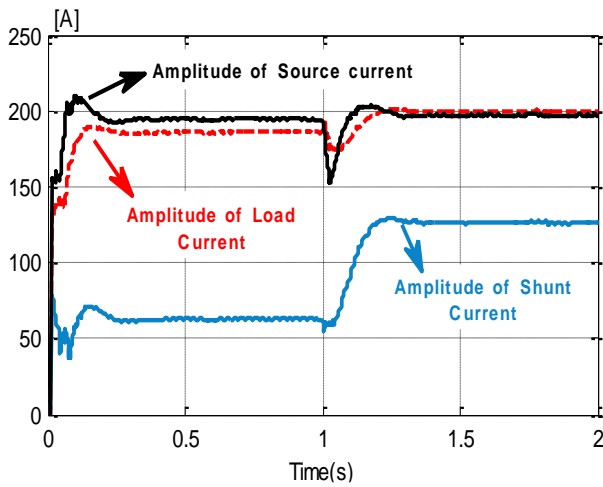


Fig. 13. Amplitudes of source current (I_L), shunt branch current (I_{sh}) and load current

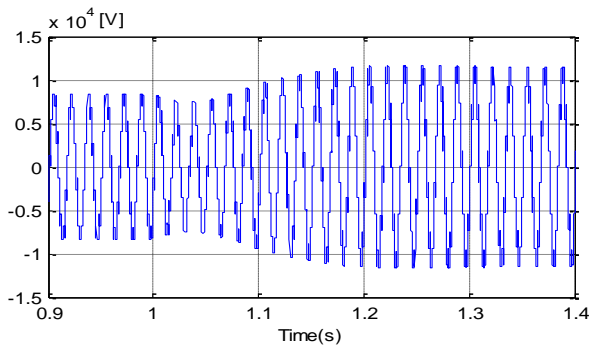


Fig. 14. Waveform of output voltage of a-phase cluster for step change of load at $t=1s$.

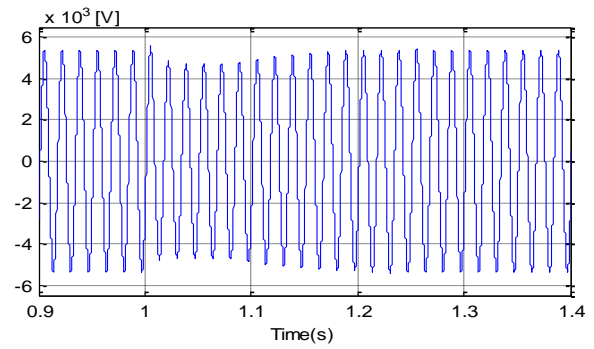


Fig. 15. Waveform of a-phase bus voltage for step change of load at $t=1s$.

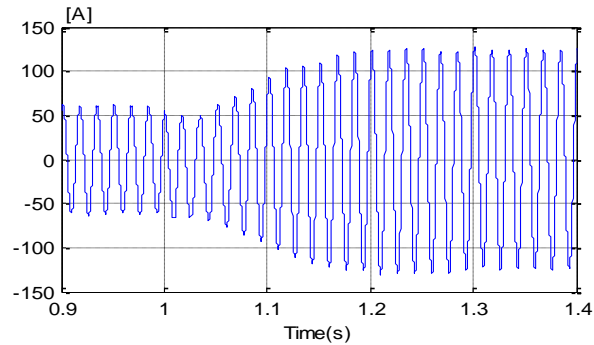


Fig. 16. Waveform of a-phase shunt current for step change of load at $t=1s$.

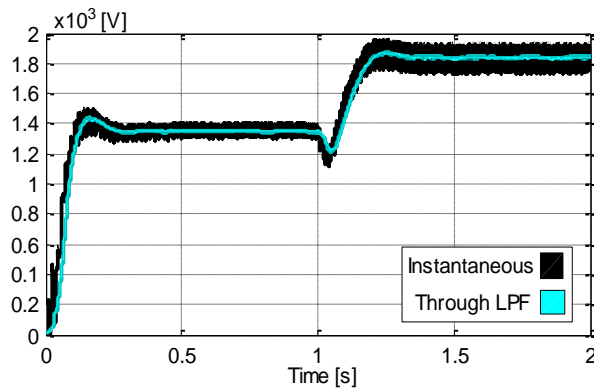


Fig. 17a

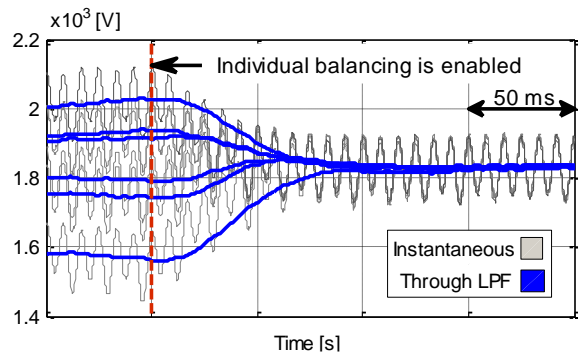


Fig. 17b

Fig. 17. DC link voltage of a-phase cluster (a) under load changes (b) with and without individual balancing

In Fig. 17b, dc link voltage balancing is started only by cluster balancing control which balances the

average value of dc link voltages and after that, individual balancing is enabled too, which modified the dc link voltages in less than 80ms without any conflict between the two control signals.

6. CONCLUSION

This paper presents a transformerless STATCOM based on a novel control algorithm for regulating a bus voltage. The control algorithm is based on single-phase instantaneous p-q power theory and "PS-PWM" modulation with carrier frequency of 1kHz. The control algorithm results from giving priority to meet reactive power demand and voltage balancing control of multiple floating dc capacitors at the same time without restriction on the cascade number. The simulation results validate the performance of the novel controller based transformerless STATCOM for voltage regulation in both aspects of generated reactive power quality and response speed.

REFERENCES

- [1] B. Singh, V. S. Kadagala, "A new configuration of two-level 48-pulse VSCs based STATCOM for voltage regulation," *Electr. Power Syst. Res.*, vol. 82, no. 1, pp. 11-17, 2012.
- [2] B. Singh, B. Singh, A. Chandra, K. Al-Haddad, "Digital implementation of an advanced static compensator for voltage profile improvement, power-factor correction and balancing of unbalanced reactive loads," *Electr. Power Syst. Res.*, vol. 54, no. 2, pp. 101-111, May 2000.
- [3] N. Bigdeli, E. Ghanbaryan, K. Afshar, "Low frequency oscillations suppression via cpso based damping controller," *J. Oper. Autom. Power Eng.*, vol. 1, no. 2, pp. 22-32, 2013.
- [4] H. Shayeghi, A. Ghasemi, "FACTS devices allocation using a novel dedicated improved PSO for optimal operation of power system," *J. Oper. Autom. Power Eng.*, vol. 1, no. 1, pp. 124-135, 2013.
- [5] R. Kazemzadeh, M. Moazen, R. Ajabi-Farshbaf, M. Vatanpour, "STATCOM optimal allocation in transmission grids considering contingency analysis in OPF using BF-PSO algorithm," *J. Oper. Autom. Power Eng.*, vol. 1, no. 1, pp. 1-11, 2013.
- [6] I. Colak, Kabalci, E., Bayindir, R., "Review of multilevel voltage source inverter topologies and control schemes," *Energy Convers. Manage.*, vol. 52, pp. 1114-1128, 2011.
- [7] E. Babaei, S. Laali, M.B.B. Sharifian, "Reduction the number of power electronic devices of a cascaded multilevel inverter based on new general topology," *J. Oper. Autom. Power Eng.*, vol. 2, no. 2, pp. 81-90, 2014.
- [8] M. Farhadi Kangarlu, E. Babaei, F. Blaabjerg, "An LCL-filtered single-phase multilevel inverter for grid integration of PV systems," *J. Oper. Autom. Power Eng.*, vol. 4, no. 1, pp. 54-65, 2016.
- [9] H. Akagi, S. Inoue, T. Yoshii, "Control and performance of a transformerless cascade PWM STATCOM with star configuration," *IEEE Trans. Ind. Appl.*, vol. 43, pp. 1041-1049, 2007.
- [10] H. Mohammadi, M. T. Bina, "A transformerless medium-voltage STATCOM topology based on extended modular multilevel converters," *IEEE Trans. Power Electron.*, vol. 26, pp. 1534-1545, 2011.
- [11] H. Akagi, H. Fujita, S. Yonetani, and Y. Kondo, "A 6.6-kV transformerless STATCOM based on a five-level diode-clamped PWM converter: system design and experimentation of a 200-V 10-kVA laboratory model," *IEEE Trans. Ind. Appl.*, vol. 44, no. 2, pp. 672-680, 2008.
- [12] M. Abbasi and B. Tousi, "Novel controllers based on instantaneous p-q power theory for transformerless SSSC and STATCOM," *In Proc. IEEE Int. Conf. Environ. Electr. Eng. Ind. Commer. Power Syst. Eur.*, Milan, Italy, 2017.
- [13] H. Stemmler, A. Beer, H. Okayama, "Transformerless reactive series compensators with voltage source inverters," *IEEE Trans. Ind. Appl.*, vol. 118, no. 10, pp. 1165-1171, 1998.
- [14] F. Z. Peng, S. Zhang, S. Yang, D. Gunasekaran, U. Karki, "Transformerless unified power flow controller using the cascade multilevel inverter," *Proc. Int. Power Electron. Conf.*, Hiroshima, 2014, pp. 1342-1349.
- [15] T. J. Hammons, "Mitigating Climate Change with Renewable and High-Efficiency Generation," *Electr. Power Compon. Syst.*, vol. 29, no. 9, pp. 849-865, 2001.
- [16] P. Gopakumar, M. J. Bharata Reddy, and D. kumar Mohanta, "Letter to the editor: stability concerns in smart grid with emerging renewable energy technologies," *Electr. Power Compon. Syst.*, vol. 42, no. 3-4, pp. 418-425, 2014.
- [17] H. Akagi, Y. Kanazawa and A. Nabae, "Generalized theory of the instantaneous reactive power in three-phase circuits," *Proc. Int. Power Electron. Conf.*, Tokyo, Japan, 1983, pp. 1375-1386.
- [18] H. Akagi, Y. Kanazawa, A. Nabae, "Instantaneous reactive power compensator comprising switching devices without energy storage components," *IEEE Trans. Ind. Appl.*, vol. IA-20, pp. 625-630, 1984.
- [19] M. Y. Lada, O. Mohindo, A. Khamis, J. M. Lazi, and I. W. Jamaludin, "Simulation single phase shunt active filter based on p-q technique using MATLAB/Simulink development tools environment," *IEEE Appl. Power Electron. Colloquium*, pp. 159-164 2011.
- [20] D. Sutanto, L. A. Snider, and K. L. Mok, "EMTP simulation of a STATCOM using hysteresis current control," *In Proc. IEEE Int. Conf. Power Electron. Drive Syst.*, Vol. 1, pp. 531-535 1999.